

# MONITORING OF AN OFFICE BUILDING IN UNINSULATED CROSS LAMINATED TIMBER CONSTRUCTION REGARDING HYGROTHERMAL COMPONENT BEHAVIOR

Nina Flexeder<sup>1</sup>, Stephan Ott<sup>1</sup>, Eva Bodemer<sup>1</sup>, Stefan Winter<sup>1</sup>

**ABSTRACT:** The use of solid timber for building construction is regulated - amongst others - by various standards regarding the physical properties of wood. In this long-term monitoring project of an office building in Austria, the relationship between the currently required theoretical target for heat transmission based on national code and the actual state of the construction is derived. The transient hygrothermal behavior of its exterior walls as well as of the different space-enclosing surfaces made of cross laminated timber (CLT) is being monitored and analyzed on the basis of everyday conditions. The focus of this paper is on the transmission heat loss through the nine-layer CLT construction which does not have any additional insulation layers. The results after one year of monitoring indicate a measured *U-value* that is lower than the one calculated according to current code. Particular attention was paid to the selection of the data in order to achieve the most accurate results possible. This shows the importance of sensor positioning, monitoring of moisture content and fairly long, undisturbed test periods with significant temperature differences between inside and outside. This paper therefore serves two purposes: It supports the proposal for a reduction in the current coefficient of thermal conductivity for CLT, and provides helpful information for future monitoring projects in order to further examine our findings.

**KEYWORDS:** monitoring, cross laminated timber, U-value, hygrothermal behavior, in-situ heat flux measurements

## 1 INTRODUCTION

### 1.1 GENERAL INFORMATION ON THE MONITORING PROJECT

Although it has been heavily researched in recent years, the knowledge about using cross laminated timber (CLT) in building construction still lacks sufficient longterm monitoring data. For the development of new guidelines, both, laboratory testing and in-situ measurements are necessary. While testing specific material parameters under defined artificial circumstances is important to gain inputs for element analysis and modeling, additional monitoring can provide data on the actual performance within a complex environment over time. Therefore, taking into account the dynamics of natural wood behavior and the complexity of building systems, further development of in-situ research at the building level is required [1-3]. By collecting extended sets of in-situ measurements regarding the interaction of indoor air quality, hygrothermal material parameters, user comfort and energy consumption, this monitoring project aims to contribute to a broad spectrum of topics in timber construction. In addition to the investigations of the building

physics behavior, the interior climate parameters and their influence on user comfort are examined using several measuring methods. For this purpose, four offices with differently clad interior CLT walls (Swiss stone pine, pine, spruce and spruce glazed) are monitored over a period of at least one year. This paper focuses on the transmission heat loss through the nine-layer CLT construction of the outer wall. All load-bearing exterior walls of the examined office building are 234 mm thick and consist entirely of CLT. These layers are glued crosswise with 1K-PU formaldehyde-free adhesive and do not have any additional insulation. The first eight layers are made of spruce, the outermost, ninth layer is larch and sealed with a solvent-based impregnation glaze (biocidal active ingredients). The inner layer is covered in a thin layer of a water-based and vapor-permeable wood stain for indoor use (acrylate dispersion).

### 1.2 RELATED STUDIES ON THE SUBJECT OF UNINSULATED CLT MONOLITHIC WALLS

If wood is used as a monolithic construction material in mainly load-bearing structures, the question of complex investigations to understand specific moisture and heat transport processes in the material often does not arise. In general, simplified thermal and hygric properties in an engineering way are sufficient to derive statements about thermal conductivity and moisture content of the material and limit considerations of damage mechanisms or (mal)-functions in building physics. For more complex problems or development projects of new technologies or products, the processes and alternating mechanisms in

<sup>1</sup> Nina Flexeder, nina.flexeder@tum.de

<sup>1</sup> Stephan Ott, ott@tum.de

<sup>1</sup> Eva Bodemer, e.bodemer@tum.de

<sup>1</sup> Stefan Winter, winter@tum.de

All: Technical University of Munich, Chair of Timber Structures and Building Construction, Germany

the material have to be investigated and understood in depth in order to be able to bring durable and save products to the market. Similar to the presented project whose measured data are shown, evaluated and discussed in this paper, the starting point for further research topics currently being investigated at the Chair for Timber Structures and Building Construction is quite the same.

This applies for example to Thermally Activated Building (TAB) components - wall components made of solid wood used to regulate the room climate by heated or cooled air inside the cross laminated timber [4-6]. Another project called "Minimal Construction" [7], is related to minimalistic construction technology that implements primarily monolithic wall or slab constructions but with a similar high level of thermal insulation as layer-wise, functionally separated constructions. By simplifying constructions and the technology; more robust and easier to dismantle and recyclable buildings are expected. The aim of the research is to apply the possibilities and limits of a conceptual minimalism concept to different types of construction, which are technically monolithic and contain few to no functional layers. Thus the exterior wall component combines several functions (load-bearing, space enclosure, air and wind tightness, heat and moisture protection). Considering climate change, effective measures must be found to reduce energy consumption and reduce greenhouse gas emissions of buildings and products. One of the central solutions is the improvement of the hygrothermal performance of the building envelope. In the research project "Minimal Construction" [7] for example, besides a mass timber construction, further construction methods namely high-insulating masonry (raw density  $\rho < 600 \text{ kg/m}^3$ ) and infra-lightweight concrete ( $\rho < 900 \text{ kg/m}^3$ ) are investigated. Due to the focus of this paper, the mass timber construction, which is the most efficient in terms of thermal performance amongst the three constructions mentioned, is the only one briefly discussed here. It remains a dilemma that with monolithic constructions in general, good hygrothermal characteristics are attainable, however for this purpose higher material consumption is necessary, than for the pure load-bearing function. Furthermore, the lowest final energy requirements of buildings, as required for passive or zero-energy houses, are difficult to achieve from a cost perspective if the construction is designed without additional insulation layers and only uses mass timber. Thus the legal minimum standard for the energy demand is achieved, but a resource efficiency in material consumption, which is mainly determined by the load-bearing function, is not fulfilled. Further dilemma remains, which is the absence of any protective inner layers, a missing installation layer, and higher direct moisture absorption of the interior surface. From the exterior, there is no weather protection cladding; compared to spruce more durable wood species are used for the exterior layer of the panel. If there is no weather protection layer, the building component is exposed to higher moisture (air humidity but also driving rain) and thus influences the moisture content in the entire component cross section as well as the thermal conductivity. This mutual influence will be shown and

discussed in the following sections based on in-situ measurement results.

### 1.3 WIDE RANGE OF THERMAL PROPERTIES FOR CLT

Depending on the average density  $\rho$  [ $\text{kg/m}^3$ ] of the wall construction, the international code ISO 10456:2007 [8] specifies the thermal conductivity  $\lambda$  [ $\text{W}/(\text{mK})$ ] by design values of  $\lambda_{450} = 0.12 \text{ W}/(\text{mK})$  (at  $\rho = 450 \text{ kg/m}^3$ ) respectively  $\lambda_{500} = 0.13 \text{ W}/(\text{mK})$  (at  $\rho = 500 \text{ kg/m}^3$ ).

Accordingly, the *U-value* [ $\text{W}/(\text{m}^2\text{K})$ ] of the outer wall used in this monitoring project is computed to be between  $U_{450} = 0.47 \text{ W}/(\text{m}^2\text{K})$  and  $U_{500} = 0.51 \text{ W}/(\text{m}^2\text{K})$ . Thus the transmission heat loss through the opaque outer walls is calculated significantly higher than the maximum number of  $U = 0.35 \text{ W}/(\text{m}^2\text{K})$ , set as the minimum efficiency target by the Austrian regulations [9]. Yet, it is assumed, that CLT may exceed the given values for thermal insulation due to its increased homogeneity (diverse orientation of growth rings, elimination of defects) and dynamic hygroscopic behavior, including latent heat effects [10, 11]. Thermal conductivity of wood, as well as lot of other material parameters depend strongly not only on the material density  $\rho$ , but also on its moisture content *MC* [%]. Similar to the correlation with density  $\rho$ , the thermal conductivity  $\lambda$  increases with moisture content *MC* of wood.

Almost 70 years ago, Kollmann [12] already declared linear correlation of thermal conductivity, density and grain direction of wood. For spruce, with a moisture content of  $MC = 12 \%$ , this results in  $\lambda_{450} = 0.114 \text{ W}/(\text{mK})$  and  $\lambda_{500} = 0.124 \text{ W}/(\text{mK})$ . Two decades later, they suggest another linear relationship, regarding moisture content *MC* [13-15]. Using the previous figures for spruce, these calculations e.g. result in the following values of decreased thermal conductivity:  $\lambda_{450, 10} = 0.111 \text{ W}/(\text{mK})$  at moisture content  $MC = 10 \%$ ,  $\lambda_{450, 8} = 0.108 \text{ W}/(\text{mK})$ ,  $\lambda_{450, 6} = 0.105 \text{ W}/(\text{mK})$ .

In recent years, the thermal properties of wooden products like CLT have been examined in several studies with steady-state conditions. Measurements with different materials used as inner layers are conducted in [10], showing great possibilities to decrease the values of thermal conductivity significantly below  $0.1 \text{ W}/(\text{mK})$ . Furthermore there are measures to improve the already low thermal conductivity of solid softwood further in mass timber panels [16] by vertical air channels of  $2 \times 18$  millimeters in section, milled in the middle layers. This product will be tested in-situ in the project mentioned previously "Minimal Construction" [7]. In [17] the use of  $\lambda = 0.092 \text{ W}/(\text{mK})$  is recommended as a new value for thermal conductivity of 3-layered CLT walls. The laboratory measurements herein reported are based on a study that showed buildings with an average moisture content of  $MC = 7.6 \%$ . Assuming this would also be the case in the present monitoring project, that would result in a corrected *U-value* lowered by 27 %. In summary, this short literature review reveals widely varying statements on the hygrothermal performance of CLT wall constructions, whereby it is noted, that in all cases the actual heat flow density was not determined in-situ.

This raises the question, if some material parameters suggested by design might not be suitable to calculate actual thermal behavior. By definition shall the design thermal values tabulated in standards like [18] resemble a ‘typical performance of that material when incorporated in a building component’ Even though this is a value derived from standardized tests, it already does account for factors like moisture content, aging and natural convection.

This paper therefore further examines the question of whether the actual dynamic thermal insulation effect of real built CLT walls might be significantly higher than the static one calculated according to today’s standards.

## 2 METHODS

### 2.1 MEASUREMENT CONCEPT

#### 2.1.1 Overview: Monitoring project

In order to assess the hygrothermal behavior of the components, a total of 154 permanent sensors were installed within the components and at in the exterior and interior surfaces. Table 1 shows the variety of measurements. Indoor comfort parameters such as room air and operative temperature, humidity, CO<sub>2</sub> content, VOC, dust and particles are also recorded and compared with the results of user surveys. The relationships between the variables and their significance for user satisfaction are identified using additional questionnaires. This paper will only address some of the data measured, primarily the heat flow and temperatures of air and material.

#### 2.1.2 Installed sensors for hygrothermal heat flow evaluation

The measurement concept includes four different office rooms, two of which are equipped with complex sensor technology in the exterior walls. One of them is oriented north, the other one serves as a comparison and faces west, like marked in figure 1. Their sensor setup is identical and as described below.

The temperature gradient within the wall is displayed by measurements of nine single sensors, distributed horizontally in the cross section of the 234 mm thick outer wall (figure 2). The resulting data points are named by their distance from the interior surface (e.g. ‘T, 40 mm’). Their values are measured by PT 1000 sensors, which were positioned in the wall during construction phase, cables pointing perpendicular to the main direction of heat flux. Thus they are parallel to the isotherms in order to avoid heat conduction through the wires. The sensors of accuracy class A are specified with a limit deviation of  $\pm (0.15 + 0.002 | t | )$  [19]. For the measured maximum temperature of 65 °C, hereinafter shown in figure 8, this corresponds to an accuracy of  $\pm 0.28$  K. Due to the four-wire circuit the effect of the wire resistance is negligible.

Two heat flux measuring plates are used to determine the heat flux density on a surface of 120 mm x 120 mm. One is placed on the outside of the massive wood wall and one on the inside. The output voltage is in the mV range and is converted into a digital signal by an analog-digital converter.

**Table 1: Ongoing building physical and health investigation, measuring cycle 5 minutes, total of 154 data points**

Temperature (air and mean radiant), relative humidity, CO <sub>2</sub> content, air velocity at each of the supply and return air spigots of the mechanical ventilation of the four offices
Temperature, relative humidity, CO <sub>2</sub> content, dust, particles, VOC; all in user proximity
Temperatures of all enclosing surfaces
Target values of the building control system
Material temperatures and material humidity (electrical resistance measurement) across the cross section of the outer wall west and north
Heat flow at both the inside and outside of the west and north exterior walls
Temperature and relative humidity of the boundary air layer on the outside of the west and north external walls
Three times VOC room air measurement in the four offices, according to DIN EN ISO 16000-3
Additional regular employee surveys with the help of a questionnaire on user comfort

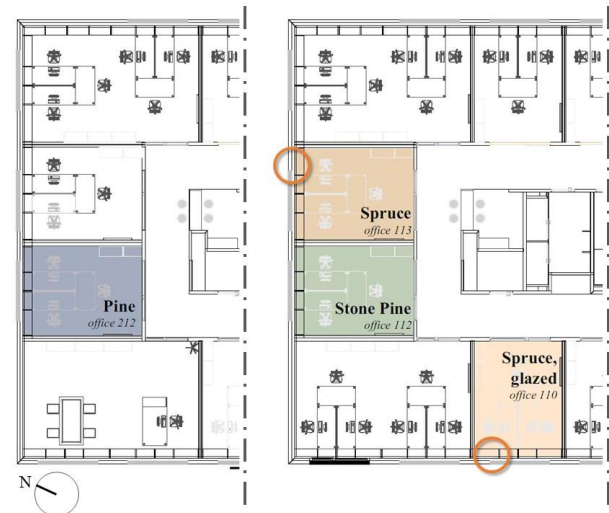


**Figure 1: 2<sup>nd</sup> Floor and 1<sup>st</sup> Floor. Three north oriented office rooms with different cladding and a reference room oriented west. The circles mark the position of the heat flux meters, exterior temperature and humidity sensors and the PT 1000 sensors, of which the results are discussed further in this paper.**

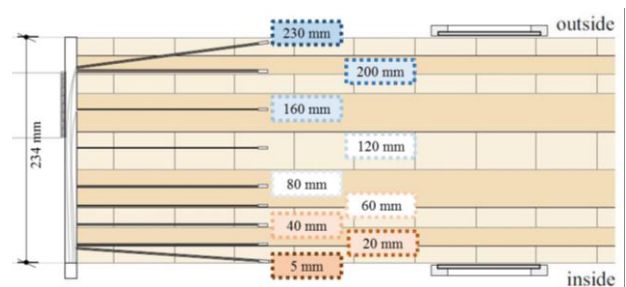


**Figure 2: Window detail, showing nine PT 1000 sensors for temperature measurements and the exterior and interior heat flux plates mounted by slender wooden frames**



**Figure 3:** Interior view of the examined CLT wall, showing the interior heat flux plate and eight pairs of electrodes (moisture monitoring through electrical resistance measurements). ©binderholz



**Figure 4:** Tripod holding a globe thermometer and a sensor measuring CO<sub>2</sub>-concentration, air temperature and relative humidity in the middle of the room. The devices are connected to the building control system via Modbus, for which the cable is led through the standpipe here. ©binderholz



**Figure 5:** Exterior view, showing another heat flux plate and a sensor for air temperature and relative humidity beneath. ©binderholz

According to the manufacturer, the accuracy of the converter (Voltage mode) reaches  $\pm 0.1\%$  or better.

The moisture content of the CLT wall is determined by the electrical resistance method. For this purpose, eight pairs of electrodes (threaded rods made of zinc-coated steel, completely insulated except for the tips) were drilled into the wall, each 30 mm apart. Due to unadjusted and therefore possibly invalid calibration curves for the used electrodes, a certain inaccuracy is to be expected. The refinement of this method is already planned in future projects. The resulting data points of each pair of electrodes are also named after their distance from the interior surface of the wall. Note that there are two different sets of temperature measurements:  $T_{si}$  and  $T_{se}$  correspond to the immediate surface temperatures of the wall, which are measured approximately 4 - 5 mm underneath the surface in this project like shown in figure 2. Although these measurements will differ slightly from the values at actual surface level, using them ensures minimized influences by heat transfer phenomena other than conduction. These values are used for measurements of the actual building element like in equation (3). In comparison  $T_i$  and  $T_e$ , like in equation (4), refer to the environmental or ambient temperature near the building element.  $T_i$  is received from the averaged measured value of the globe thermometer and the air temperature sensor installed in the middle of the room (“resultant” or “comfort temperature”, as in [20], Annex A.3.3b), shown in figure 4. The exterior temperature  $T_e$  is measured by an air temperature sensor, which is mounted outside on the façade, in immediate vicinity of the other measurements, shown in figure 5.

## 2.2 ANALYSIS OF HEAT TRANSFER THROUGH EXTERIOR WALL

### 2.2.1 Main assessment of thermal transmittance

In general, the  $U$ -value is used to rate an outer shell in regards of its insulation properties and therefore serving as an important benchmark for evaluating a building’s energy efficiency. According to [8,18] the  $U$ -value in this case is calculated using a design value of thermal conductivity of  $\lambda = 0.13 \text{ W/(mK)}$ , at  $\rho = 500 \text{ kg/m}^3$ , with an internal surface resistance of  $R_{si} = 0.13 \text{ m}^2\text{K/W}$  and an external surface resistance of  $R_{se} = 0.04 \text{ m}^2\text{K/W}$  to  $U = 0.51 \text{ W/(m}^2\text{K)}$  using equation 1:

$$U = \frac{1}{R_T} = \frac{1}{R_{si} + R + R_{se}} = \frac{q}{T_i - T_e} \quad (1)$$

where  $U$  = thermal transmittance [ $\text{W/(m}^2\text{K)}$ ],  $R_T$  = total thermal resistance [ $\text{m}^2\text{K/W}$ ],  $R_{si}$  = internal surface thermal resistance [ $\text{m}^2\text{K/W}$ ],  $R_{se}$  = external surface thermal resistance [ $\text{m}^2\text{K/W}$ ],  $T_i$  = interior ambient temperature [ $^{\circ}\text{C}$ ] or [ $\text{K}$ ],  $T_e$  = exterior environmental temperature [ $^{\circ}\text{C}$ ] or [ $\text{K}$ ] and  $q$  = density of heat flow rate [ $\text{W/m}^2$ ].  $R$  = thermal resistance of the building element [ $\text{m}^2\text{K/W}$ ] and can be derived using equation 2:

$$R = \frac{T_{si} - T_{se}}{q} = \frac{1}{\Lambda} = \frac{d}{\lambda} \quad (2)$$

where  $T_{si}$  and  $T_{se}$  are the interior respectively exterior surface temperatures of the building element [°C] or [K],  $A$  = thermal conductance of the building element [W/(m<sup>2</sup>K)],  $d$  = thickness of the layer [m] and  $\lambda$  = thermal conductivity of the material [W/(mK)].

Instead of using standardized design values, in this paper the  $U$ -value is computed based on the specifically measured values for  $\lambda$  and juxtaposed to the actual measured transmittance  $U$  (where possible). Those values are then compared with the ones derived from standards, theoretical literature and other measurement projects. Especially for further projects it might be of great interest to notice, that the correct evaluation of in-situ measurements requires specific conditions meeting statistical requirements (see the following chapters).

### 2.2.2 Analysis using the Average Method

The thermal resistance of the exterior wall  $R$  [m<sup>2</sup>K/W], its reciprocal, the thermal conductance  $A$  [W/(m<sup>2</sup>K)] and, derived from the element's thickness  $d$  [m], the thermal conductivity  $\lambda$  [W/(mK)] are calculated adhering to the *Average Method* described in [20]:

$$R = \frac{\sum_{j=1}^n (T_{sij} - T_{sej})}{\sum_{j=1}^n q_j} = \frac{1}{\Lambda} = \frac{d}{\lambda} \quad (3)$$

with  $T_{si}$  and  $T_{se}$  meaning the interior respectively exterior surface temperatures of the building element [°C] or [K] and  $q$  = density of heat flow rate [W/m<sup>2</sup>]. The index  $j$  enumerates the individual measurements up to the end of a test period after  $n$  steps. The  $U$ -value [W/(m<sup>2</sup>K)] is derived accordingly, with  $T_i$  = interior and  $T_e$  = exterior ambient temperature [°C] or [K]:

$$U = \frac{\sum_{j=1}^n q_j}{\sum_{j=1}^n (T_{ij} - T_{ej})} \quad (4)$$

Depending on the specific heat per unit area, different approaches for data acquisition are recommended. The thermal capacity  $C$  [J/m<sup>2</sup>K] of the examined CLT wall is calculated by using a material density of  $\rho = 500$  kg/m<sup>3</sup>, and a thickness of  $d = 0.234$  m.

$$C = \rho \cdot c \cdot d \quad (5)$$

While Radmanović and Đukić suggest a mean specific heat capacity  $c = 1.2$  kJ/kgK for wood fibers [21], Adl-Zarrabi and Boström calculate a value of  $c = 1.49$  kJ/kgK for spruce [22] and the international standard ISO 10456:2007 specifies the value  $c = 1.6$  kJ/kgK for plywood [8], the German code DIN 4108-4:2017-03 generally names the value of  $c = 2.1$  kJ/kgK for timber and wood-based materials [23]. Although the calculated thermal capacity  $C$  of the examined wall varies widely, depending on the values used as specific heat capacity  $c$ , it will exceed the definition of  $C > 20$  kJ/(m<sup>2</sup>K) by a factor of 7 to 12.

Hence, in order to obtain an asymptotical value close to the real  $U$ -value, the conditions for heavier elements shall be met. Albeit different periods will be examined in Chapter 3, the duration  $D_T$  of the test will always be an

integer multiple  $INT$  of days [d], so in this case start and end time are always at 8:00 AM. The tests conducted shall exceed a required minimum of 72 h and fulfill the following three conditions on statistical accuracy, where consistency of the value  $R$  is proofed:

- A) Deviation of the  $R$ -Value obtained at the end at the test  $R_t$  from the  $R$ -Value  $R_{t-24h}$  obtained 24 h before, like shown in figure 6.

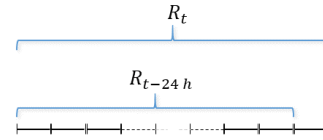


**Figure 6:** Condition A - comparison of the  $R$ -value from the end of the test period with the value from 24 hours before

- B) Deviation of the  $R$ -Value  $R_{DT1}$  obtained from the first time period during  $INT (2 D_T/3) d$  and the value  $R_{DT2}$  from the last time period with the same duration, like shown in figure 7.

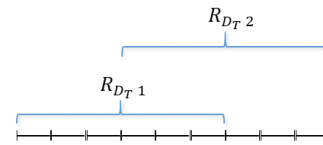


**Figure 7:** Condition B - comparison of the  $R$ -value from the first two thirds end of the test period with the  $R$ -value from the last two thirds

- C) Fraction: The change of heat stored in the wall in comparison with the amount of heat passed through the wall over  $D_T$ . This condition depends on the value used for mean specific heat capacity  $c$ . For simplicity,  $c = 1.6$  kJ/kgK is assumed in the following evaluation.

$$\frac{C}{\Lambda \cdot D_t} = \frac{\rho \cdot c \cdot d}{\sum_{j=1}^n q_j} \cdot (t_n - t_1) \quad (6)$$

The results of all three conditions, A, B and C, shall not exceed a value of 5 %. If these conditions cannot be fulfilled, the computed estimate for  $R$  (and related parameters  $A$ ,  $\lambda$  and  $U$ ) are considered misleading.

### 2.2.3 Further examination of highly fluctuating data

In this paper two additional methods are used for smoothing the resulting curve of any time-dependent value  $x(t)$  and to show its tendencies. The simple moving average (SMA) shows the mean value of  $x(t_k)$  of the past 72 h for any point in time  $t_k$ , using the last 864 rows of data each, therefore  $m = 864$ . The result of equation (7) is then plotted for each  $t_k$ .

$$SMA(t_k) = \frac{1}{m} \sum_{j=0}^{m-1} x(t_{k-j}) \quad (7)$$

Furthermore, the cumulative moving average (CMA) observes any convergences to an asymptotical value since start of a test period, after  $k$  steps:

$$CMA(t_k) = \frac{1}{k} \sum_{j=1}^k x(t_j) \quad (8)$$

At the end of a test with  $n$  steps,  $k = n$ .

### 2.2.4 Investigation of possible influences specific to this monitoring project

Regardless of the manufacturer's information on device accuracy, the heat flux measurements are expected to be influenced by the following factors:

- Alignment of devices: Falsification of the measurement results due to poor sensor position
- Significance of data: Inaccuracies due to insufficient measured value amplitude
- Unwanted user interaction: Interference from human presence or other electronic devices (e.g. PCs, phones,..) close by

As there is a multitude of data available by now, picking the right test period should avoid these factors.

First, it is noted, that in general a temperature gradient is the driving potential for any heat flow. Possible distortions of the heat flux meter outputs are examined by analysis of correlations of sensor data and solar irradiation in different scales.

Second, simply based on the underlying mathematical term for calculating  $R$ ,  $U$  and other related parameters, accuracy will increase with a greater temperature difference between inside and outside. Both, the temperature difference of  $T_{si} - T_{se}$  in the north and the west wall, as well as  $T_i - T_e$  in the north oriented room are analyzed by using equation (7).

And third, the presence of office workers and the associated electromagnetic interference voltages, higher internal heat gains and manual interventions in the building's air conditioning are suspected to greatly influence all hygrothermal measurements.

In order to gain knowledge about the possible falsification of heat flux measurements by human interaction, periods of usual office hours, reduced office hours (Lockdown 2020) and no office hours at all (holidays) are identified using the data of the motion detectors and the CO<sub>2</sub>-sensors installed.

## 3 RESULTS: MEASUREMENTS OF HEAT TRANSFER

### 3.1 DETECTION OF INFLUENCES BY DEVICE ALIGNMENT

The ongoing project has been collecting about  $10^7$  data points since summer of 2019, so that there are continuous year-round sets (sample rate: 5 minutes) of material and air temperature, as well as heat flux measurements by now. Figure 8 shows the resulting temperature distribution within the wall cross-section for a typical west and a typical north wall. By zooming in, to a shorter time period of five exemplary days, the relevance of the orientation to the sky and the phase shift during the solar heating process is shown in figure 9. Due to direct irradiation, heat-flow density through the west wall from the outside is up to 10 times greater than at the north side of the building. In addition, heat fluxes at the outer layer, both north and west, are oscillating strongly, which can be attributed to the higher external convection. At both exterior walls mean measured heat fluxes from the interior into the construction show a characteristic day-night shift and are considerably lower than the mean heat flux from the construction back into the interior space. Clearly, solar radiation has a large impact on all measured data and possibly distorts the heat flux measurements especially at the exterior surface of the west wall. According to [20], clause 6.1, heat flux meters and other relevant temperature sensors should be protected from exposure to direct sunlight. Hence the data of the exterior west wall should be carefully selected (night time, cloudy weather), which severely limits the measurement period available for evaluation by methods described in chapter 2. The measurements of a period of 365 days are used to compute the values shown in table 2. Please note, that both exterior heat flux measurements do not meet the conditions for accuracy and therefore are only shown for educational purposes. The office oriented west does not have a tripod measuring air and global temperature in the middle of the room, which is why the  $U$ -value cannot be measured in this case. It can, however, be calculated using the actual measured value for thermal conductivity  $\lambda$  of the material in equations (1, 2).

**Table 2: Evaluation of the dynamic heat flow measurements for a whole year and four differently placed heat flux meters**

	$R$ [m <sup>2</sup> K/W]	A condition [%]	B condition [%]	C condition [%]	$A$ [W/(m <sup>2</sup> K)]	$\lambda$ [W/(mK)]	$U$ [W/(m <sup>2</sup> K)]
North, interior	1.885	0.08	2.52	1.12	0.530	0.111	0.427
North, exterior	1.375	0.34	45.92	-	0.727	0.153	0.585
West, interior	1.951	0.15	3.03	1.16	0.513	0.108	-
West, exterior	0.851	0.33	52.67	-	1.174	0.247	-

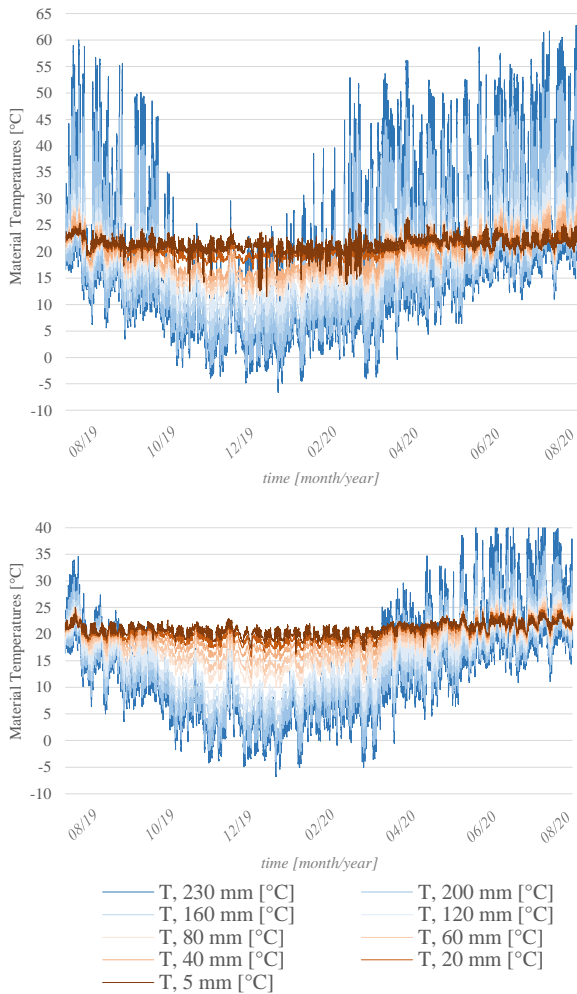


**Figure 8:** Year-long temperature measurements in western (top) and northern outer walls

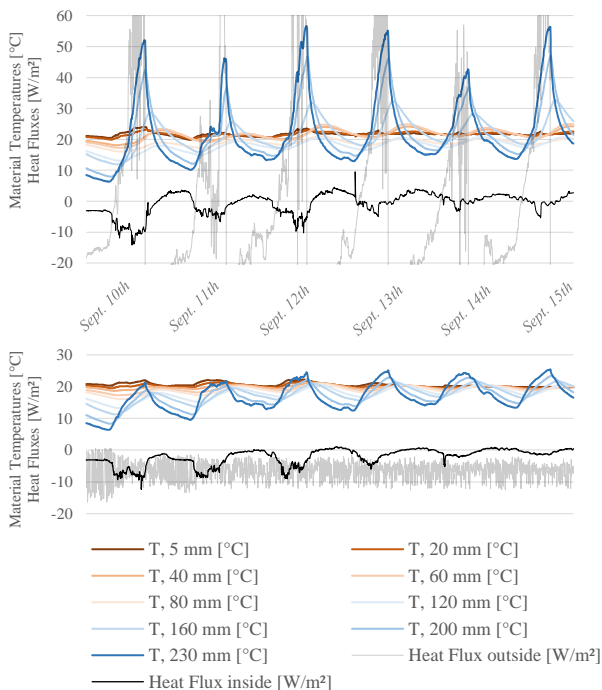


**Figure 9:** Exemplary temperature measurements in western (top) and northern outer walls as well as heat flow measurements for September 10<sup>th</sup> to September 15<sup>th</sup> 2019

### 3.2 INCREASED ACCURACY BY SELECTION OF DATA

Picking specific seasons for testing can increase the significance of data while reducing the required amount of measurements at the same time. In [24] different approaches for in-situ measurements are compared with best results shown by the heat flux measurements using a minimum temperature difference of at least 10 Kelvin. Figure 10 (west office) and figure 11 (north office) show the time span, when this condition is fulfilled. The exterior wall of the west office is heated by solar irradiation for most time of the year, causing the temperature differences between inside and outside to mostly drop below 10 K. In the year of August 2019 – August 2020, there is only a time span of 87 days remaining, where the rule of  $\Delta T_s \geq 10$  K can be fulfilled.

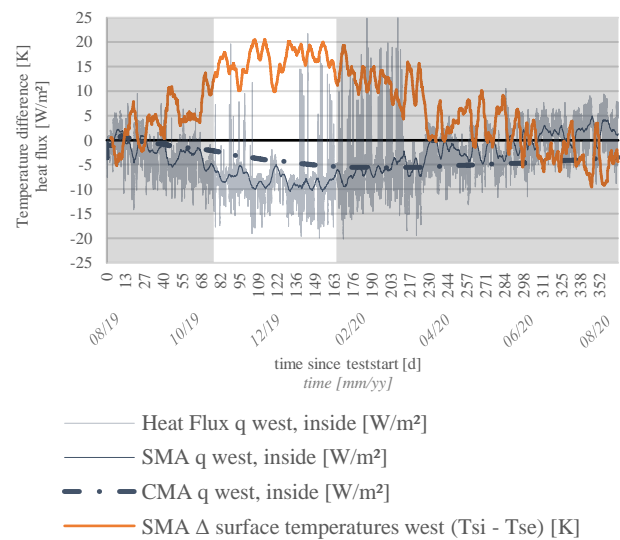


**Figure 10:** Application of the rule  $\Delta T_s \geq 10$  K, leaving a relatively narrow window for evaluation of the measurements obtained in the west wall

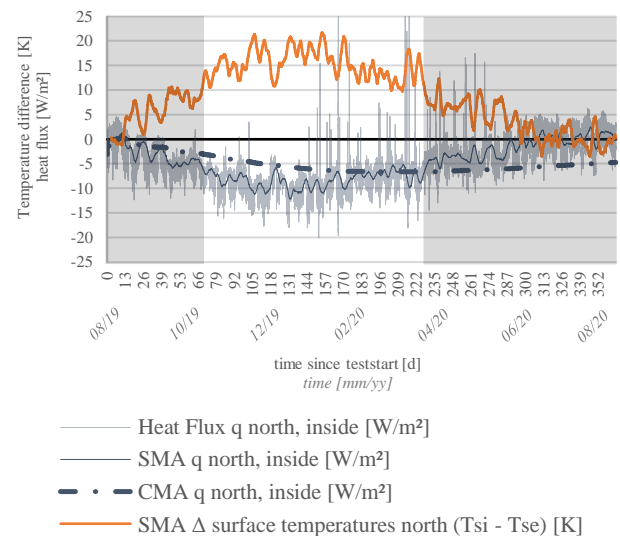


**Figure 11:** Application of the rule  $\Delta T_s \geq 10$  K, leaving a significantly wider window for evaluation of the measurements obtained in the north wall

**Table 3: Evaluation of the dynamic heat flow measurements for a time span, where  $\Delta$  surface temperatures ( $T_{si} - T_{se}$ )  $\geq 10$  K, and with two differently placed heat flux meters**

	$R$ [m <sup>2</sup> K/W]	A condition [%]	B condition [%]	C condition [%]	$\lambda$ [W/(m <sup>2</sup> K)]	$\lambda$ [W/(mK)]	$U$ [W/(m <sup>2</sup> K)]
North, interior	1.845	0.02	0.51	2.49	0.542	0.114	0.456
West, interior	1.993	0.16	3.21	5.18	0.502	0.105	-

Assessment of the north wall, however proofed to be much more convenient, offering a remaining window of evaluation, which is nearly twice as wide (159 days). The results for the north office in table 3 show improved values for condition A and B, indicating an almost perfect convergence. The elevated deviation for condition C, however, displays the importance of longer test periods. As the time span of great differences is significantly shorter at the west wall, these results do not appear with the same accuracy. Based on this example and depending on the thermal capacity of the examined construction as well as the local climate, a minimum of at least 90 days is recommended for in-situ heat flow measurements, preferably in the coldest season of the year.

### 3.3 EXCLUSION OF USER-RELATED DISTURBANCES

Under normal conditions, each of the examined office rooms is used by three employees, sitting at a desk with a computer, several screens, phones and other technical equipment, in a 1-2 m distance to the inner heat flux plate. For the 17-day time period in December 2019 – January 2020, when no relevant amounts of CO<sub>2</sub>-production were measured, the examined office was unoccupied. Thus the heat flux measurement is assumed to have no faulty measurements caused by human interaction.

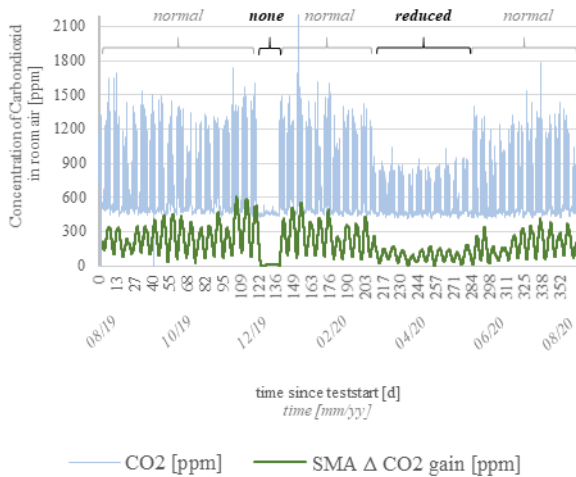


**Figure 12: Analysis of carbon dioxide emissions in the north oriented office, concluding to: office hours = none / reduced / normal**

**Table 4: Evaluation of the dynamic heat flow measurements for a time span of specific office use and two differently placed heat flux meters**

	$R$ [m <sup>2</sup> K/W]	A condition [%]	B condition [%]	C condition [%]	$\lambda$ [W/(m <sup>2</sup> K)]	$\lambda$ [W/(mK)]	$U$ [W/(m <sup>2</sup> K)]
North, interior, none	1.827	0.55	0.08	16.44	0.547	0.115	0.462
North, interior, reduced	1.862	0.38	3.27	5.09	0.537	0.113	0.419
West, interior, none	2.028	0.20	2.15	18.25	0.493	0.104	-
West, Interior, reduced	1.906	0.10	5.42	5.21	0.525	0.110	-

Due to the rather short time span, condition C cannot be met, resulting in inaccurate values. The partial Lock-down in March – June 2020 resulted in another period of specific interest for undisturbed measurements. In these months the offices were used by only a reduced number of staff, which can be deducted from very low values of CO<sub>2</sub>-production, like in figure 12 and were validated by the measurements of the air spigots (mechanical ventilation), motion sensors as well as confirmed by employees. For the resulting converged values for measurements with reduced office hours please refer to table 4.

## 4 DISCUSSION

### 4.1 COMPARISON OF DIFFERENTLY COMPUTED RESULTS

Depending on the chosen data set used, there is a total of six different asymptotical values for  $R$ , all of which meet the statistical requirements in chapter 2. The number and variance of these computed values are very project-specific and are mainly shown to demonstrate the range of measurement. As the values for the thermal resistance of the exterior wall  $R$  [m<sup>2</sup>K/W] differ by around 8 %, the values for the thermal conductivity  $\lambda$  [W/(mK)] of the material CLT also show slightly fluctuating results, like in figure 14.

Possible reasons for any fluctuations might be small differences in material, minor inaccuracies in the measuring devices used, undetected user influences or other disturbances not related to the actual hygrothermal behaviour of CLT. The actual physical influence of the moisture content is therefore discussed below.

### 4.2 INFLUENCES BY MOISTURE CONTENT

The computed mean values for the moisture content in each wall, north and west, are shown in figure 13. They vary, depending on depth and season. In summary, for the examined period of September 2019 to September 2020, the north wall had an average moisture content of 9.7 %, with a slight upward trend. For the same time

span, the west wall shows a slight downward trend and an average of  $MC = 9.2\%$ . The details of the temperature dependent moisture determination method as well as the dynamic gradient in the component cross-section (depending on the glued layers) do hold further influences on the hygrothermal behavior. These topics shall not be discussed further in this paper, but merely indicate subjects for future in-depth research. Using the correlation methods mentioned in chapter 1 [12-15], these moisture contents would result in a MC modified  $\lambda_{450, 9.2} = 0.1098 \text{ W/(mK)}$  and  $\lambda_{450, 9.7} = 0.1105 \text{ W/(mK)}$ ;  $\lambda_{500, 9.2} = 0.1192 \text{ W/(mK)}$  and  $\lambda_{500, 9.7} = 0.1199 \text{ W/(mK)}$  respectively.

### 4.3 OVERALL COMPARISON OF STANDARDIZED, CALCULATED AND MEASURED VALUES

When comparing differently derived results for the  $U$ -value of the north wall, an estimate of  $U = 0.4375 \pm 0.0185 \text{ W/(m}^2\text{K)}$ , based on a thermal conductivity of  $\lambda = 0.111 \pm 0.005 \text{ W/(mK)}$  would show great similarity with all measured values in this project (like in figure 15). Thus the theoretical value, modified to a density of  $\rho = 450 \text{ kg/m}^3$  and a moisture content of  $MC = 9.7\%$ , by the findings of [12-15],  $\lambda_{450, 9.7} = 0.1105 \text{ W/(mK)}$  would describe the actual real value of thermal conductivity very well. The values measured by [10] are derived at a significantly higher moisture content, but result in similar figures around  $\lambda \approx 0.09 - 0.11 \text{ W/(mK)}$ .

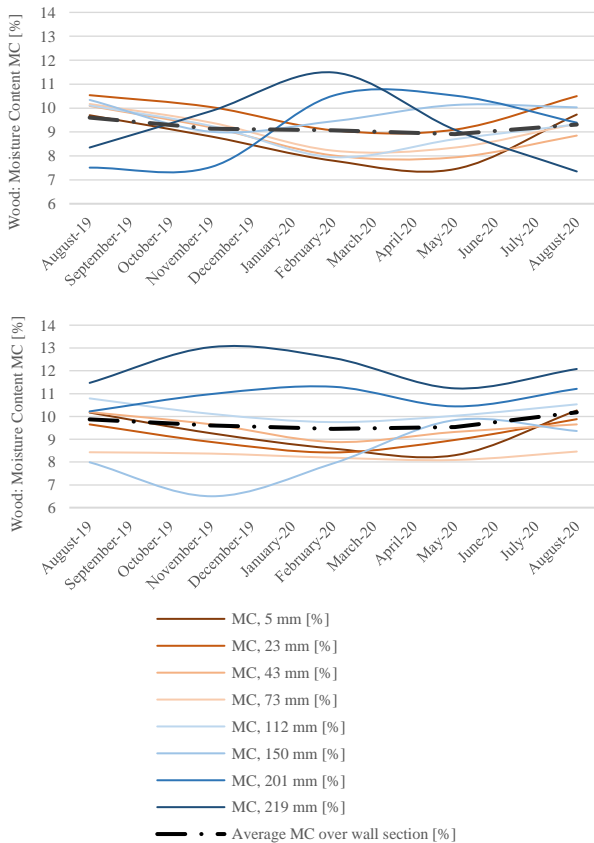


**Figure 13:** Year-long results for moisture content MC, based on electrical resistance measurements in western (top) and northern outer wall

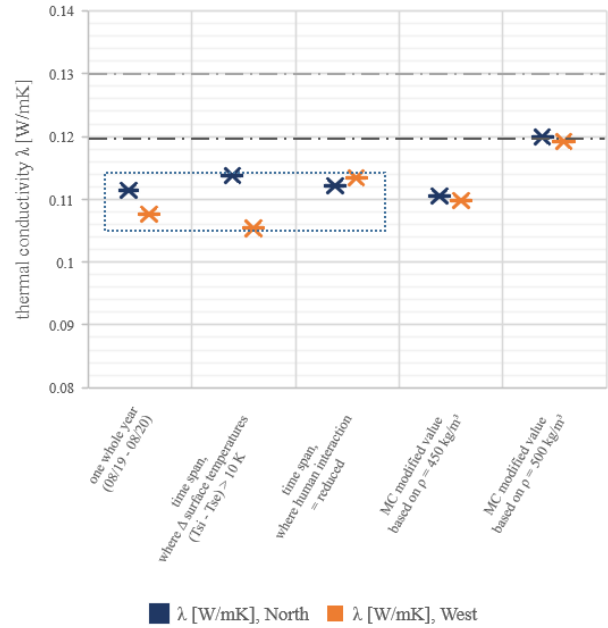


**Figure 14:** Comparison of varying values for thermal conductivity  $\lambda$  [W/(mK)]: Computed results from different approaches in chapter 2 and 3 are paired with the MC modified values according to chapter 1. Only statistically valid results are shown.

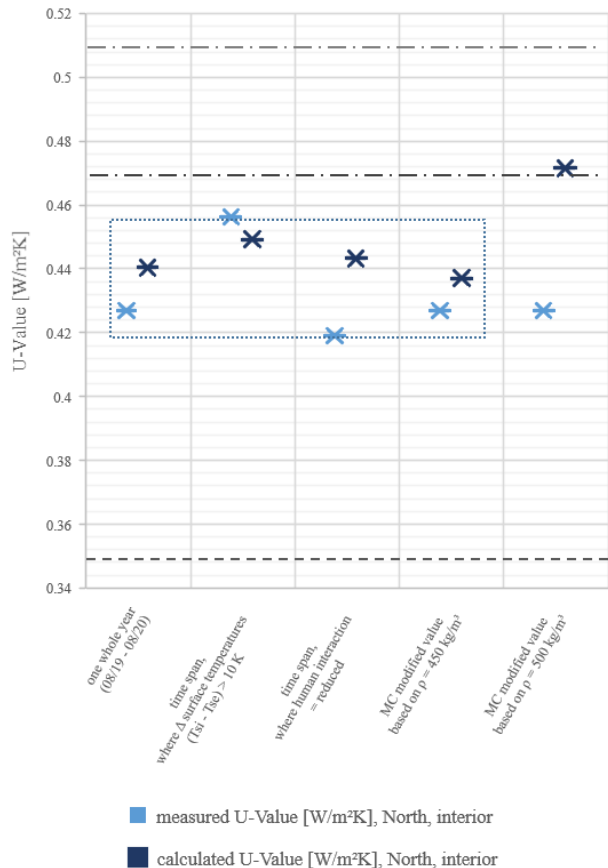


**Figure 15:** Comparison of varying values for thermal transmittance  $U$  [W/(m<sup>2</sup>K)]: Computed and actually measured results from different approaches in chapter 2 and 3 are paired with the U-values based on the MC modified values according to chapter 1 (figure 14).

## 5 CONCLUSIONS

The *U-value* (measured and calculated), as well as the value for thermal conductance of CLT are significantly better than the ones, provided as standards for softwood timber. Based on the monolithic walls of a real office building, a value of  $\lambda = 0.111 \pm 0.005$  W/(mK) shows a significantly better fit than the values determined by today's code. It is noted, that thermal conductivity of wood (like a lot of other materials as well) increases with higher temperatures. This issue is not addressed in this paper, yet it may have an impact at exterior walls like the ones examined [10, 22]. Another future field of research will be the improvement of the moisture measurement technology used, which has a sensitive influence on the possible mathematical modification of the value for thermal conductivity  $\lambda$  [W/(mK)]. In general, this paper aims to not only contribute to the knowledge about thermal properties of wooden products, but also encourage others to conduct in-situ measurements. Therefore, information on how to obtain statistically valid thermal measurements are elaborated. The monitoring project presented here is still to be continued and further results on long-term hygrothermal behavior are expected in the future. Besides that, there are further goals, especially concerning user comfort. By evaluating the dependencies of building physics, room climate determining parameters and volatile organic compounds (VOCs), in connection with a regular anonymous user survey, general optimization potentials for the planning of office buildings in solid timber construction shall be developed.

## ACKNOWLEDGEMENT

The project *BBS Thermo TimberBrain*, in Hallein (AT) was sponsored by Binderholz Bausysteme GmbH. Thanks are especially offered to Christof Richter.  
<https://bit.ly/313z8CH>

## REFERENCES

- [1] Pei S., Rammer D., Popovski M., Williamson T., Line P., van de Lindt J. W.: An Overview of CLT Research and Implementation in North America. In: *World Conference on Timber Engineering*, 2016.
- [2] Schmidt E. L., Riggio M., Laleicke P. F., Barbosa A. R., Van Den Wymelenberg K.: How monitoring CLT buildings can remove market barriers and support designers in North America: An introduction to preliminary environmental studies. In: *CLEM+CIMAD*, 2017.
- [3] Schmidt E. L., Riggio M.: Monitoring Moisture Performance of Cross-Laminated Timber Building Elements during Construction. *Buildings* 9, no. 6: 144.
- [4] Mindrup K, Winter S.: Thermal activation of solid timber elements for indoor climate control. In: *World Conference on Timber Engineering*, 2018.
- [5] Mindrup K.: Room climate conditioning using thermally activated solid timber elements. PhD Thesis, Technical University of Munich, 2020.
- [6] Kornadt O., Carrigan S., Schöndube T., Winter S., Mindrup K., et. al.: Dynamic thermal-hygric behaviour of solid constructions - Development of a heat storage capacity index for buildings made of masonry and thermally activatable solid timber elements. *Forschungsinitiative Zukunft Bau*, 2019.
- [7] Nagler et. al.: Minimal Construction. *Forschungsinitiative Zukunft Bau*, 2018.
- [8] Building materials and products - Hygrothermal properties - Tabulated design values and procedures for determining declared and design thermal values (ISO 10456:2007 + Cor. 1:2009); German version DIN EN ISO 10456:2010-05 + AC:2009.
- [9] Österreichisches Institut für Bautechnik, OIB-Richtlinie 6: Energieeinsparung und Wärmeschutz, OIB-330.6-009/15, 2015.
- [10] Niemz P., Sonderegger W.: Untersuchungen zur Wärmeleitung von Vollholz und Werkstoffen auf Vollholzbasis, wesentliche Einflussfaktoren. In: *Bauphysik*, vol. 33, no. 5, p. 299-305, 2011.
- [11] Liu F., Jia B., Chen B., Geng W.: Moisture transfer in building envelope and influence on heat transfer. In: *10th International Symposium on Heating, Ventilation and Air Conditioning*, 2017.
- [12] Kollmann F.: Technologie des Holzes und der Holzwerkstoffe. Springer-Verlag Berlin Göttingen Heidelberg, 1951.
- [13] Kollmann F.: Poren und Porigkeit in Hölzern. In: *Holz als Roh- und Werkstoff*, no. 45, p. 1-9, 1987.
- [14] Forest Products Research Society: Wood Handbook. In: *Agric. Handbook*, no. 72, 1974.
- [15] Niemz, P., Sonderegger W.: Holzphysik – Physik des Holzes und der Holzwerkstoffe. Carl Hanser Verlag München, 2017.
- [16] ETA 13/0643. DoP Starkholzelemente (english: mass timber panels), ARS Starkholzplatten GmbH. 2019.
- [17] Griesebner L. M., Egle, J.: Salzburger Holzbau 2020+, RWF-Kooperationsprojekt, 20102-719/162/2013, 2013.
- [18] Building components and building elements - Thermal resistance and thermal transmittance - Calculation methods (ISO 6946:2017); German version DIN EN ISO 6946:2018-03.
- [19] Industrial platinum resistance thermometers and platinum temperature sensors (IEC 60751:2008); German version DIN EN 60751:2009-05.
- [20] Thermal insulation - Building elements - In-situ measurement of thermal resistance and thermal transmittance - Part 1: Heat flow meter method, ISO 9869-1:2014-08.
- [21] Radmanović K., Đukić S.: Specific Heat Capacity of Wood. In: *Drvna Industrija*, vol. 65, no. 2, p. 151-157, 2014.
- [22] Adl-Zarrabi B., Boström L.: Determination of Thermal Properties of Wood and Wood Based Products by Using Transient Plane Source. In: *8th World Conference on Timber Engineering*, 2004.
- [23] Thermal insulation and energy economy in buildings - Part 4: Hygrothermal design values; German version DIN 4108-4:2017-03.
- [24] Desogus G., Mura S., Ricciu R.: Comparing different approaches to in situ measurement of building components thermal resistance. In: *Energy and Buildings*, vol. 43, no. 10, p. 2613-2620, 2011.